Topographical Distribution of Perioperative Cerebral Infarction Associated with Transcatheter Aortic Valve Implantation

Abbreviated Title: TAVI-related brain infarct distribution

Jonathon P. Fanning, BSc, MBBS [1,2,3]; Allan J. Wesley, MB ChB, FRANZCR [3,4]; Darren L. Walters, MBBS, MPhil, FRACP, FCSANZ, FSCAI [2,3,5]; Andrew A. Wong, MBBS, PhD, FRACP [3,6]; Adrian G. Barnett, BSc, PhD [1,7]; Wendy E. Strugnell, BAppSc (MIT) [4]; David G. Platts, BMedSci, MBBS, MD, FRACP, FCSANZ, FESC, FASE [1,2,3,5]; John F. Fraser, MB ChB, PhD, FRCP (Glasgow), FFARCSI, FRCA, FCICM [1,3,8]

[1]The Critical Care Research Group, The Prince Charles Hospital, Brisbane, Australia

[2]The Heart & Lung Institute, Metro North Hospital and Health Service, Brisbane, Australia

[3]The University of Queensland, Brisbane, Australia

[4]Department of Medical Imaging, The Prince Charles Hospital, Brisbane, Australia

[5]Department of Cardiology, The Prince Charles Hospital, Brisbane, Australia

[6]Department of Neurology, The Royal Brisbane and Women's Hospital, Brisbane, Australia

[7]School of Public Health, Queensland University of Technology, Brisbane, Australia

[8]Adult Intensive Care Unit, The Prince Charles Hospital, Brisbane, Australia

Corresponding author: Jonathon P Fanning, Critical Care Research Group, The Prince Charles Hospital, Rode Road, Chermside, Brisbane, Queensland 4032, Australia. Telephone: +61 7 3139 6880. Fax: +61 3139 6120. Email: Jonathon_fanning@me.com

Total word count: 5,806 words (title page: 214; abstract: 250; body: 3,864; acknowledgements, contributions, disclosures and funding sources: 193; references: 1,272).

Abstract

Background: Transcatheter aortic valve implantation (TAVI) is associated with a high incidence of cerebrovascular injury. As these injuries are thought to be primarily embolic, neuroprotection strategies have focussed on embolic protection devices. However, the topographical distribution of cerebral emboli and how this impacts on the effectiveness of these devices has not been thoroughly assessed. Here, we evaluated the anatomical characteristics of magnetic resonance imaging (MRI)-defined cerebral ischaemic lesions occurring secondary to TAVI to enhance our understanding of the distribution of cardioembolic phenomena.

Methods: Forty patients undergoing transfemoral TAVI with an Edwards SAPIEN-XT^{TM} valve under general anaesthesia were enrolled prospectively in this observational study. Participants underwent brain MRI pre-procedure, and 3±1 days and 6±1 months post-procedure.

Results: Mean±standard deviation participant age was 82±7 years. Patients had an intermediate-to-high surgical risk, with a mean Society of Thoracic Surgeons score of 6.3±3.5 and EuroSCORE of 18.1±10.6. Post-TAVI there were no clinically apparent cerebrovascular events but MRI assessments identified 83 new lesions across 19/31 (61%) participants, with a median±inter-quartile range number and volume of 1±2.8 lesions and 20±190µL per patient. By volume, 80% of the infarcts were cortical, 90% in the posterior circulation and 81% in the right hemisphere.

Conclusions: The distribution of lesions that we detected suggests that cortical grey matter, the posterior circulation, and the right hemisphere are all particularly vulnerable to perioperative cerebrovascular injury. This finding has implications for the use of intraoperative cerebral embolic protection devices, particularly those that leave the left subclavian and, therefore, left vertebral artery unprotected.

Introduction

Transcatheter aortic valve implantation (TAVI) has revolutionised the management of severe aortic stenosis in patients at high surgical risk. However, neurological events remain a concerning complication with clinically apparent stroke occurring in as many as 9.1% of patients in the early postoperative period.[1,2] Furthermore, the perioperative incidence of magnetic resonance imaging (MRI)-defined cerebral infarcts ranges from 58–91%.[3-12]

The aetiology of neurological injury associated with TAVI is multifactorial but thromboembolic phenomena arising from the procedure are understood to be primarily responsible. An analysis of embolic protection devices removed following TAVI procedures found that 99% of filters contained embolic debris, including thrombus, calcification, valve tissue, arterial wall and foreign material.[2] Thus, embolic protection devices have become the 'new frontier' of both TAVI-related and perioperative neuroprotection research.

As MRI-defined cerebral infarcts are common and can be objectively and specifically measuremed, they have become an accepted surrogate marker of perioperative cerebral embolisation and a recommended primary endpoint to determine neuroprotection device efficacy.[13, 14] Although a number of studies have reported the incidence of these lesions following TAVI,[3-12] few explore their anatomical distribution, which is essential for understanding emboli transport and the subsequent cerebral predilection for injury. Here, we used diffusion-weighted MRI (DWI) lesion number and volume to characterise the topographic pattern of cerebral ischaemic lesions following the TAVI procedure. The distribution that we identified not only extends our understanding of the causative mechanisms of cerebrovascular injury but also allows us to assess the effectiveness of current

neuroprotective strategies.

Materials and Methods

Study design and patient selection

Prospective, consecutive screening was performed on all patients presenting to The Prince Charles Hospital in Brisbane, Australia for isolated TAVI using the SAPIEN-XT™ (Edwards LifeSciences, Irvine, CA, USA) via a transfemoral approach between January and December 2016. Each patient's suitability for TAVI was determined by a multidisciplinary 'heart team', which included cardiologists (general, interventional, and imaging), a cardiothoracic surgeon, a cardiac anaesthetist, and nursing staff, as per international guidelines.[15] In all patients, TAVI was performed under general anaesthesia, induced with propofol and maintained with sevoflurane, neuromuscular blockade (cisatracurium or rocuronium), and an ultra-/short-acting opioid (remifentanil or fentanyl). Depth of anaesthesia was guided by Bispectral Analysis (BIS™, Covidien, Dublin, Ireland).

Before subject recruitment or data collection, ethics approval was obtained from the hospital's Human Research Ethics Committee (HREC/12/QPCH/291). Informed consent was obtained from all participants prior to their enrolment in the study. All-comers were considered with exclusion criteria as follows: (1) pre-existing neurological impairment, as defined by a modified Rankin score of ≥3 (i.e., moderate disability, requiring some assistance, but able to mobilise independently); (2) previous cerebrovascular events (including stroke or transient ischaemic attack); (3) carotid artery stenosis >50% on duplex ultrasonography; (4) the presence of intra-cardiac thrombus identified on routinely performed pre-procedure transoesophageal echocardiograph; (5) any contraindication to magnetic resonance imaging (MRI), including incompatible metallic prosthesis or foreign body, the inability to lie flat, or claustrophobia requiring sedation; (6) poor to absent English-speaking

skills; and (7) prior aortic valve replacement.

Imaging

At baseline (within 24 hours prior to TAVI), an MRI of each patient's brain was obtained using a 1.5-Tesla system (MAGNETOM Aera, Siemens Healthcare GmbH, Erlangen, Germany). These scans were used to assess cerebrovascular anatomy, identify significant intracranial stenosis, and grade degenerative changes in each patient. The Global Cortical Atrophy Scale (GCAS) was used to quantify the degree of cerebral atrophy,[16] and the Fazekas scale to quantify T2 hyperintense lesions in periventricular white matter and deep white matter.[17] Early follow-up MRI was performed on post-procedure day 3±1, and those who sustained cerebral infarction were followed-up with a repeat MRI at 6±1 months. The imaging protocol for the baseline assessment was comprehensive, consisting of standard fast-spin echo sequences (T1-weighted and T2-weighted), DWI, apparent diffusion coefficient (ADC) mapping, susceptibility-weighted imaging (SWI), T2-weighted fluid-attenuated inversion recovery (FLAIR), and time of flight angiography of the Circle of Willis to document any pre-existing disease. The more limited follow-up scans comprised DWI, ADC, SWI, T2-weighted, T1-weighted, and FLAIR imaging. Cerebral ischaemia was defined by DWI hyperintensity caused by the restricted diffusion of water with reciprocal hypointensity on ADC maps.[18] T1-weighted, T2-weighted, and FLAIR sequences were used to exclude other lesions that can mimic strokes. Lesions were quantified both by number and by volume, the latter using automated three-dimensional reconstructions from planimetry obtained by manual contouring (OsiriX, Geneva, Switzerland). To analyse their topographical distribution, lesions were stratified based on the type of brain parenchyma involved, hemisphere, and vascular territory (Figure 1).
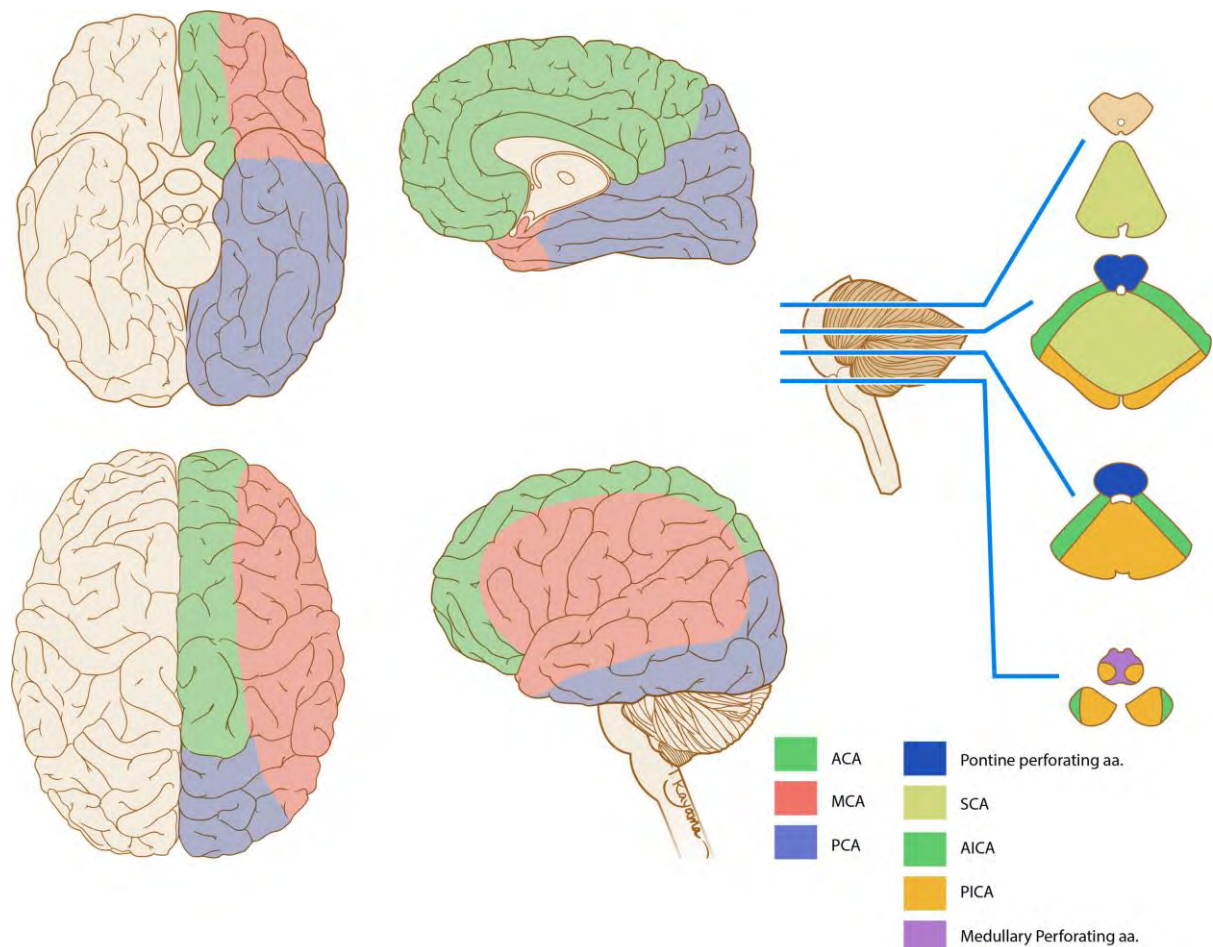
Figure 1: Vascular territories of the brain. aa, arteries; ACA, indicates anterior cerebral artery; AICA, anterior inferior cerebellar artery; MCA, middle cerebral artery; PCA, posterior cerebral artery; PICA, posterior inferior cerebellar artery; SCA, superior cerebellar artery. © Kayama Studios 2016.

Clinical assessment

A detailed standardised medical history was obtained from each patient. Clinically apparent stroke was detected and localised using the National Institutes of Health Stroke Scale (NIHSS), whereas the modified Rankin Scale was used to categorise stroke severity. These tests were administered within 24 hours prior to the TAVI procedure, and again at 3±1 days, 6±1 weeks, and 6±1 months post TAVI.

Statistical analysis

The primary endpoint was new DWI-positive lesions on the post-procedure scan relative to baseline MRI, quantified by both number and volume (μL).[13, 18] Clinically apparent cerebrovascular events, including stroke (either major or minor) and transient ischaemic attack (TIA), were secondary endpoints. Summary statistics are presented as means±standard deviations (SD) when the data were parametric, or as medians±inter-quartile range (IQR) when non-parametric. Significance testing was performed for both: (1) the null hypothesis (N_0) that distribution is equal (i.e., 50:50 between anterior:posterior circulations [$P_{50:50}$]); and, (2) the N_0 that the number of embolic lesions is proportional to blood flow, which is weighted 70:30 anterior:posterior circulations [$P_{70:30}$]).

Results

Patient and procedural characteristics

Forty patients were enrolled between January and December 2016, and are included in this

analysis. A flowchart of patients throughout the study is shown in Figure 2. Baseline patient
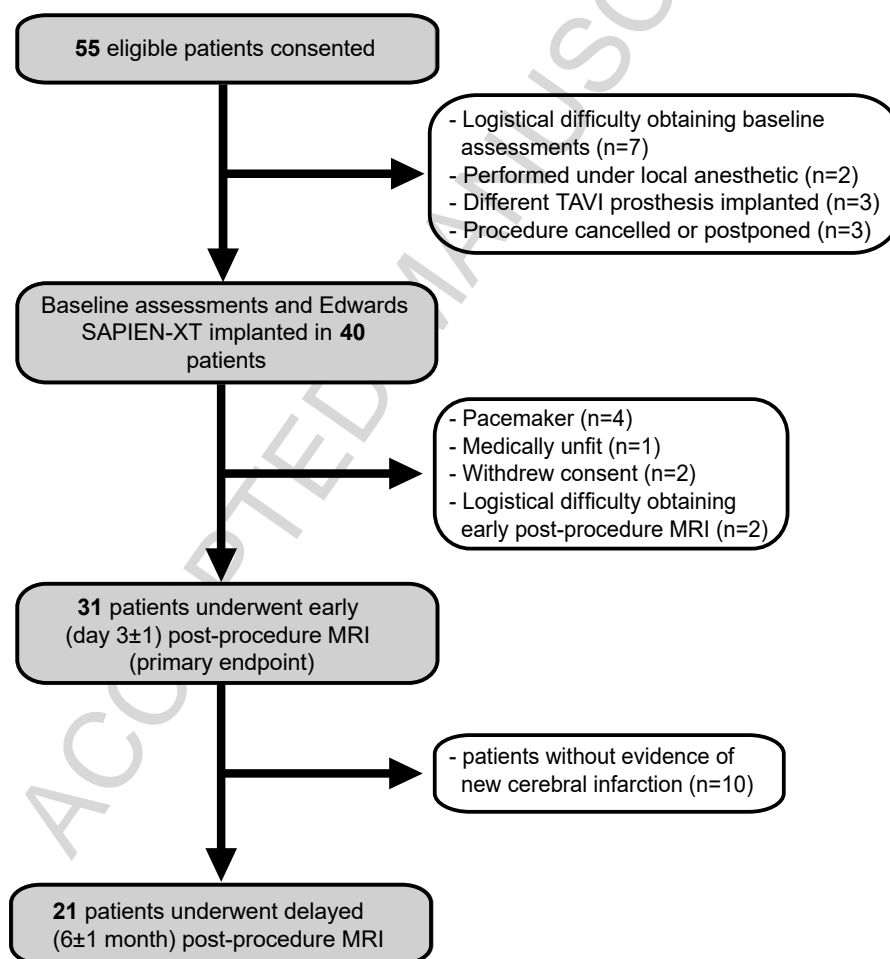
and procedural characteristics are summarised in Table 1.[15]

Figure 2: Flowchart of study participants.

Variable	Measure
Patient Characteristics (n=40)	
Age, years	82.3 ± 7
Female	24 (58.5)
Logistic EuroSCORE, %	18.06 ± 10.6
STS score, %	6.27 ± 3.5
BMI, kg/m^2	28.8 ± 7.2
Hypertension	32 (78%)
Hyperlipidemia	36 (88%)
Diabetes mellitus	16 (39%)
Chronic renal impairment	12 (29%)
Chronic lung disease	12 (29%)
Significant (>5 pack year) smoking	18 (44%)
Pre-operative LVEF	57.8 ± 14.05
Atrial fibrillation	12 (29%)
Procedural Characteristics	
Device success	38 (95%)
Average procedure time, minutes	73.1 ± 35.9
Average fluoroscopic time, minutes	14.2 ± 8.3
Fluoroscopy contrast volume, mL	146 ± 50

Table 1. Baseline characteristics. Values are expressed as mean ± SD or as n (%). Abbreviations: BMI, body mass index; LVEF, left ventricular ejection fraction; STS, Society of Thoracic Surgeons.

Neurologic outcomes

Baseline MRI

Given the advanced age and moderate-to-high risk of the study population, it is not surprising that a degree of global cerebral atrophy was identified in all patients on baseline MRI (Figure 3). In two patients, a subacute supratentorial infarct was detected: one exhibited a deep white matter infarct, and the other a cortical infarct. Convincing chronic MRI evidence of seven

prior infarctions was observed across five individuals. Focal SWI hypointensity was observed in the majority (32/40) of patients. A total of 90 lesions were identified, with a median of 2±2.25 lesions per patient. In addition, SWI sequences identified gyriform superficial siderosis in three individuals and linear evidence of previous haemorrhagic change in an old infarct in another patient. One-quarter of the patients (10/40) had persistent foetal origins of their posterior cerebral arteries (PCAs), whereby the posterior communicating artery was greater in calibre than the ipsilateral P1 segment of the PCA. Incidental findings included a pituitary macroadenoma, a pontine cavernous angioma, a 4mm right internal carotid artery aneurysm, and the recurrence of a meningioma resected approximately two decades earlier.
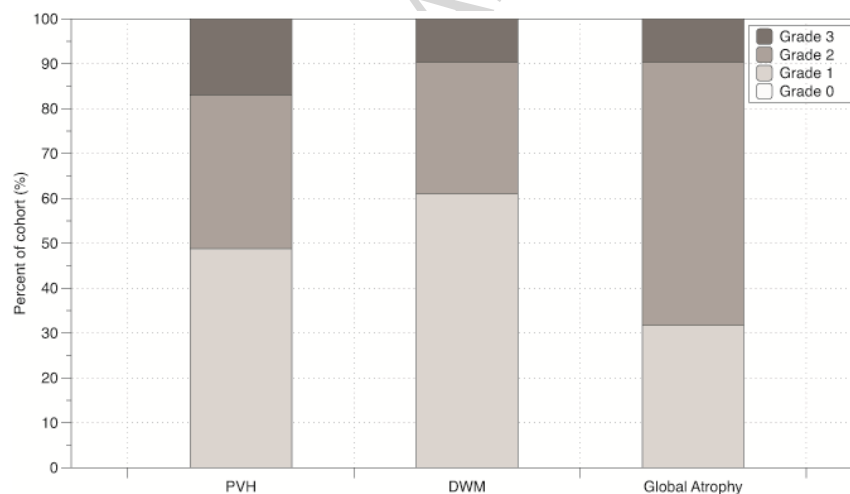

Figure 3: Radiological grading of degenerative changes using the Global Cortical Atrophy Scale (Global Atrophy), and Fazekas scores for periventricular white matter (PVH), and deep white matter (DWM).

Post-procedural MRI

Of the 40 participants who underwent a baseline MRI and received a SAPIEN-XT valve, 31 were assessed for the primary endpoint (Figure 2). We identified 83 new DWI-positive lesions across 19/31 (61%) patients, a median of 1±2.8 lesions/patient, with a volume of 20±190 μL/patient. In those 19 patients, typically more than one lesion was present (in 12/19 cases; 63%). The distribution characteristics of these lesions are presented in Table 2 and Figure 4. Lesions typically involved the cortical grey matter by both number (50 lesions or

60%) and volume (9,327 µL or 80%) and 49 (59%) occurred in the posterior circulation and 34 (41%) in the anterior circulation ($P_{50:50} = 0.2$; $P_{70:30} < 0.0001$). Similarly, when considering the total volume of infarction, 10,255 µL (90%) occurred in the posterior compared with 1,192 µL (10%) in the anterior circulation ($P < 0.0001$ for both N_0). By number, 43 (63%) lesions occurred in the right hemisphere versus 25 (37%) lesions on the left ($P = 0.06$) totalling volumes of 9,250 µL (81%) and 2,150 µL (19%), respectively ($P < 0.0001$). Importantly, cerebellar and brainstem lesions were not lateralised to the left or right as such stratification would confound our understanding of the distribution of cardiogenic emboli traversing the aorta and branches.

Fifteen lesions demonstrated a T2-FLAIR or T1-weighted signal abnormality, which can be ascribed to the relatively small average infarct size to slice thickness. Four acute infarcts in three patients demonstrated new, associated SWI hypointensity consistent with haemorrhage. Eighteen new post-procedural SWI hypointensities were identified in ten patients, with a maximum of four new lesions per patient. Superficial linear gyral SWI hypointensity suggestive of low-volume subarachnoid haemorrhage was identified in one patient.
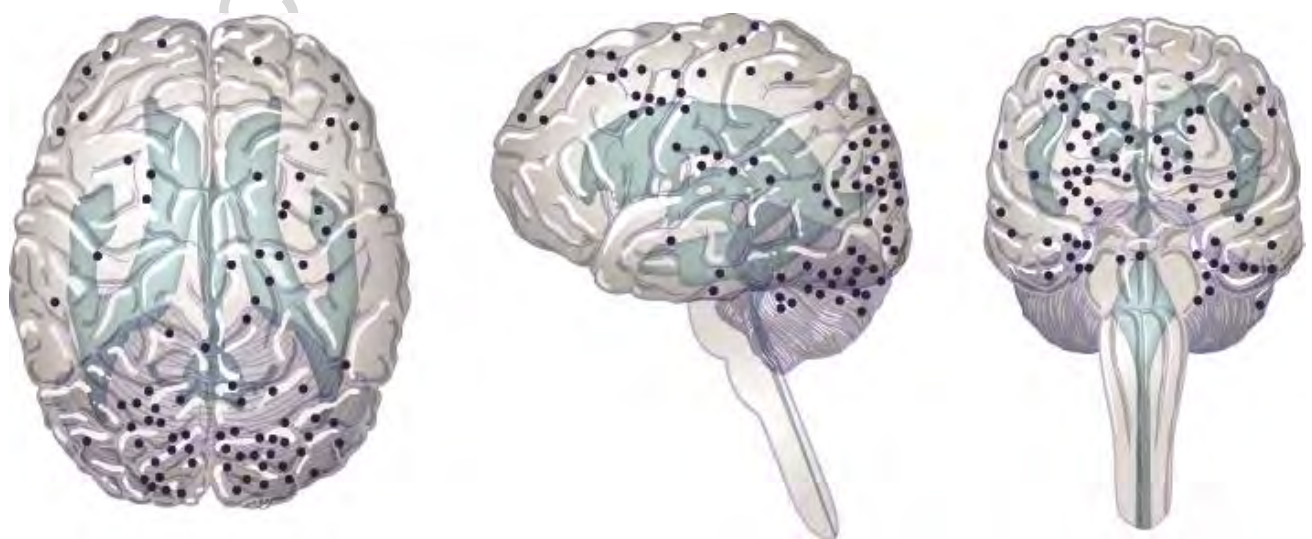

Figure 4: Anatomical distribution of MRI-defined cerebral infarctions in three-dimensional views of the brain: A) sagittal, B) coronal, and C) axial. © Kayama Studios 2016.

	Number of lesions	P-value	Total volume of lesions (µL)	P-value
Hemispheric Distribution (excluding cerebellum and brainstem)				
Right	43 (63%)	0.06	9250 (81%)	<0.0001
Left	25 (37%)		2150 (19%)	
Vascular Distribution				
Anterior Circulation	34 (41%)	0.2*; <0.0001[†]	1192 (10%)	<0.0001*[†]
Posterior Circulation	49 (59%)		10255 (90%)	
Brain Parenchyma				
Cortical Grey	50 (60%)		9327 (80%)	
Subcortical Grey	3 (4%)		185 (2%)	
Subcortical White	15 (18%)		782 (7%)	
Cerebellar	13 (16%)		1106 (10%)	
Brainstem	2 (2%)		220 (2%)	

Table 2. Anatomical distribution of MRI-defined cerebral infarctions. * Based on the null hypothesis that emboli distribution is equal (i.e., 50:50); [†] Based on the null hypothesis that emboli distribution is proportional to blood flow (which is weighted 70:30 anterior:posterior).

Six-month MRI

All post-procedural DWI-positive lesions resolved by the 6-month MRI scan consistent with the natural evolution of DWI changes. Given the relatively small volumes of the infarcts, the majority of lesions were no longer reliably detectable on T2-FLAIR or T1-weighted sequences. One individual demonstrated new SWI hypointensity at an infarct site and three new SWI hypointensities were detected in another patient. A new linear superficial gyriform SWI hypointensity, consistent with blood products, in a third individual. Finally, a new acute left-frontal, deep white matter infarct was identified in an individual with advanced background white matter changes at baseline.

Objective clinical assessments

No clinically apparent cerebrovascular events were detected.

Discussion

This analysis offers a unique opportunity to observe the distribution of cardiogenic microemboli and new ischaemic lesions post-TAVI. We identified 83 new lesions across 19/31 (61%) participants, 80% of which by volume involved cortical grey matter, 90% occurred in the posterior circulation and of those occurring in the anterior circulation, 81% were in the right hemisphere. This topographical distribution raises several procedural and physiological questions for consideration.

TAVI is associated with the frequent occurrence of cerebral ischaemic lesions, with reported incidence rates ranging from 58–98%.[3-9, 19] The 61% incidence identified in this cohort is at the lower end of this range and could reflect the comparatively lower surgical risk of this sample and also the continual improvement in TAVI prostheses and procedures.[20] Indeed, the SAPIEN-XT valve used in this study has now largely been superseded by a newer-generation iteration, the SAPIEN-3, which has demonstrated lower risk for cerebral infarction generation.[2]

Considering vascular territories, significantly greater cerebral infarction was observed in the posterior versus anterior circulation with the PCA territory being the most vulnerable. This result is perhaps counter-intuitive as emboli should favour arteries that receive the largest volume of blood. The anterior cerebral circulation is formed by branches of the internal carotid arteries and in healthy awake patients contributes approximately 70% of the brain's blood supply.[21] The remaining 30% of cerebral blood flow arises from the two vertebral arteries, and this is the major supply for the posterior cerebral circulation. Based on blood

flow distribution, therefore, one-third of all cardiogenic emboli would be expected in the posterior circulation. Consistent with this, when considering all strokes, typically only 20–25% of ischaemic events occur in the posterior circulation.[22]

Blood-flow distribution during cerebrovascular stress is less clear. The influence of anaesthesia is of particular relevance but is poorly characterised with limited studies presenting conflicting data. Indeed, its effect is likely to be heterogeneous depending on the exact drugs, dosage and area of brain considered. Kaitsi *et al*.[23] identified a global reduction in cerebral blood flow (propofol > sevoflurane in equianaesthetic doses); however, significant dose-dependent regional differences were evident. For example, high doses (2 minimum alveolar concentration [MAC]) of sevoflurane concurrently caused noticeable increased cerebellar flow (38%) and reduced frontal flow (23%). Conversely, Rozet *et al*.[24] using low dose sevoflurane anaesthesia (0.5 MAC) demonstrated that posterior circulation blood flow was reduced relative to the anterior circulation.

Inextricably linked to cerebral blood flow are the cerebral autoregulation and neurovascular coupling mechanisms that defend the brain against haemodynamic and metabolic disturbance. Impaired autoregulation may result in relative hyper- or hypoperfusion, either of which could be detrimental. Specifically, increased blood flow might deliver more emboli, whereas reduced blood flow could magnify the effects of microemboli by impairing their washout.[25] Thus relatively impaired cerebral autoregulation in the posterior versus anterior circulation is a plausible explanation for the observed differences in vulnerability to injury. This is supported by the findings that (1) the posterior circulation has lower carbon dioxide reactivity than the anterior circulation,[26] and (2) there is impaired dampening of arterial blood pressure oscillations in the posterior versus the anterior circulation.[27] Again, the role of

anaesthesia is unclear with Rozet *et al*.[24] providing the only data and in only low dose sevoflurane (0.5 MAC) anaesthesia where cerebrovascular reactivity was maintained in both anterior and posterior circulations.

Anatomical differences also exist between the anterior and posterior circulations and may contribute to or explain some of the abovementioned physiological characteristics and vulnerability of the posterior circulation. Fluorescence microscopy of adult human brain tissue has identified differences in sympathetic innervation of the anterior versus posterior cerebral arteries with clear implication for vascular tone and autoregulatory capacity.[28] Furthermore, insult / injury may be exacerbated by intracranial atherosclerosis, which is more prone to occur in the posterior than anterior circulation, with the basilar artery being the single most common site.[29] The tortuous path of the vertebral arteries and acutely angled branches of the basilar artery might exacerbate this predilection further (Figure 5).
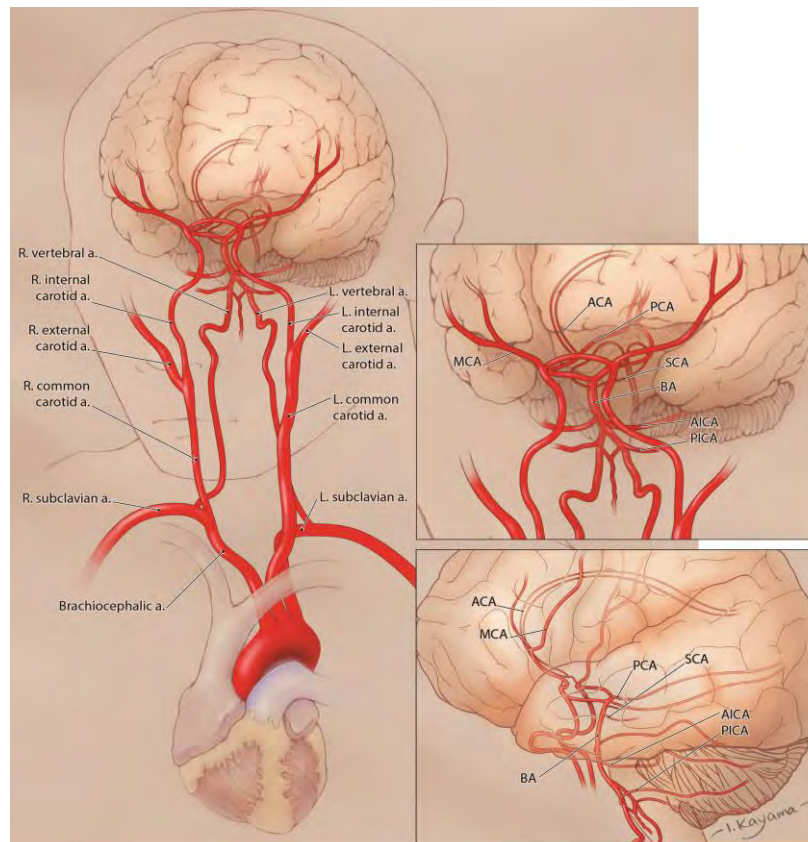
Figure 5: Anatomy of the cerebral circulation. R indicates right; L, left; a, artery; aa, arteries; ACA, anterior cerebral artery; AICA, anterior inferior cerebellar artery; MCA, middle cerebral artery; PCA, posterior cerebral artery; aa, arteries; PICA, posterior inferior cerebellar artery; SCA, superior cerebellar artery. © Kayama Studios 2016.

Alternatively, the distribution of cerebral infarcts may reflect differences in distribution of embolic load / insult rather than innate regional anatomical or physiological differences. Sophisticated modelling has shown a size-dependent trajectory for cardiogenic emboli reaching the carotid and vertebral arteries that varies distinctly from what is expected based on blood flow distribution.[30] In particular, the preponderance of small to medium-sized cardiogenic particles reaching the branch arteries of the aortic arch, and subsequently the carotid and vertebral arteries, was markedly greater than that expected using volumetric flow.[30] However, further stratification of emboli between the carotid and vertebral arteries was not assessed.

A preponderance of clinically apparent infarctions in the posterior regions of the brain in patients undergoing cardiac surgery[31-35] and TAVI[3, 4, 7] has been noted previously, albeit not consistently.[5, 8-11] Cassie *et al* also documented this predilection experimentally. In a supine canine model and using an antifoam solution to perfuse the aorta, these investigators identified a significantly greater number of emboli and infarcts in the cerebellum, brainstem, and occipital lobes.[36]

Logically, the effects of gravity must also be considered in supine patients who receive large doses (average 140mL in our patient cohort) of iodinated radio-contrast during fluoroscopy. The density of radio-contrast used in this setting is greater than that of whole blood, a characteristic that is essential to its utility. Consequently, it is feasible that a contrast bolus might preferentially pool posteriorly in a supine patient, thereby reducing the oxygen-carrying capacity of the blood or drawing disproportionate emboli. However, this postulation is purely speculative.

In our patient cohort, the right hemisphere seemed to be more vulnerable than the left, accounting for 63% of the ischaemic lesions by number ($P_{50:50}$=0.06; $P_{70:30}$ < 0.0001) and 81% by volume (P<0.0001 for both N_0). This is contrary to other TAVI studies, in which lesions were predominately in the left cerebral hemisphere.[4, 6, 8, 9] The left-sided vulnerability observed in these early studies was proposed to result from exposure of the left common carotid to emboli dislodged from the aortic arch during the placement and use of catheters and associated devices. However, transcranial Doppler studies have reported the majority of embolic signals arising while the TAVI prosthesis is being positioned and implanted and have concluded that the major source of embolic burden is the aortic valve itself.[37] It is important to recognise that embolic signals as measured by transcranial Doppler in this study

did not discriminate the nature or size of embolic material or indicate a threshold for emboli sufficient to cause infarction.

The right-sided vulnerability that we observe seems more logical because as cardiogenic emboli traverse the aortic arch, the innominate artery supplying the right hemisphere is the first to be encountered; thus, it is exposed to the total embolic load whereas subsequent supra-aortic arch vessels are exposed to a lesser load. Furthermore, anatomically, the innominate artery is of larger calibre and traverses a course parallel to the ascending aorta, contrary to the left carotid artery, which is smaller and arises perpendicular to the aortic arch.[38]

We identified 60% of the lesions by number and 80% by volume in the cortical grey matter. Although the threshold for ischaemia is often considered and reported on a whole-brain basis, tissue-specific differences support increased vulnerability of grey over white matter. Perhaps most evident are differences in the cellular constituents and, therefore, metabolic requirements and blood flow,[39] as well as well-documented differences in neurochemical responses to ischaemia.[40] MRI studies have also established a significantly lower ischaemic threshold in grey versus white matter, with a cut-off for cerebral blood flow of 35 versus 20 mL/100 g/min ($P < 0.0001$) and a cerebral blood volume of 1.7 versus 1.2 mL/100 g, respectively ($P < 0.0001$).[41] Consequently, grey matter has greater blood flow and volume, and a shorter mean transit time than white matter; thus, the former may be exposed to greater embolic loads and be more vulnerable to hypoperfusion.

The topographical distribution of new ischaemic lesions that we observed has implications for neuroprotection during TAVI. Studies to date suggest that embolic protection devices

represent a promising adjunct for improving the safety of TAVI. Recently published randomised controlled trials of the Sentinel[TM] Cerebral protection System [Claret Medical, Santa Rosa, CA, USA] have shown a reduction in the volume of MRI-detected cerebral infarction in vascular territories protected by embolic protection devices resulting in FDA approval.[2, 19, 42-44] However, this and other cerebral protection devices – e.g., the Embrella[TM] embolic deflector system [Edwards Lifesciences Ltd., Irvine, CA, USA] – are inefficient at protecting the left subclavian artery (Figure 6). This is the origin of the left vertebral artery, which merges with the right vertebral artery to form the basilar artery – the major supply to the posterior portion of the Circle of Willis (Figure 5). Thus, embolic protection devices that lack coverage of the left subclavian artery also fail to completely protect the posterior circulation resulting in 19 of 28 vascular territories and 26% of the brain volume being either partially or completely unprotected.[19] Our findings highlight this territory as one of the most vulnerable to ischaemic lesions suggesting that, although technically challenging, the development of embolic protection devices that offer full coverage of all three supra-aortic branches of the aortic arch may be beneficial.
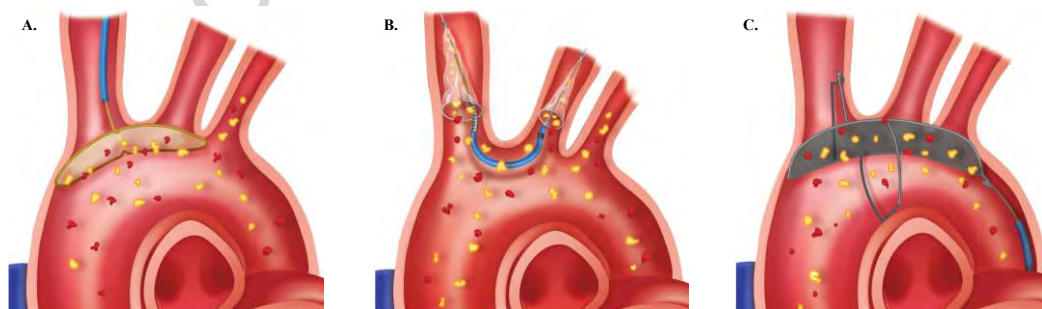

Figure 6: Embolic protection devices. A) Embrella[TM] Deflector (Edwards LifeSciences, Irvine, CA, USA); B) Sentinel[TM] cerebral protection system (Claret Medical, Santa Rosa, CA, USA); C) Triguard[TM] Cerebral Deflector (Keystone Heart Ltd, Caesarea, IL, USA). Reprinted from Fanning *et al.*[1] with permission of the publisher. © 2014, Elsevier, Inc.

Our study involved only a relatively small, nonrandomised patient cohort and all the TAVI

procedures were performed exclusively using the Edwards SAPIEN-XT^{TM} prosthesis, limiting extrapolation of these findings to newer iterations of TAVI prostheses or other cardiac procedures. Furthermore, the risk stratum of our cohort was heterogeneous, with a mixture of intermediate-risk, high-risk, and inoperable participants. Although comparing differences in surgical risk strata is prudent, this was not possible for our cohort. The limited sample size and high incidence of DWI-positive lesions also affected our ability to perform more sophisticated logistic regression analysis. DWI and neurologic assessments were performed conscientiously, however, they were only possible in those patients able to tolerate them. Several of our TAVI patients were unable to undergo follow-up scans due to frailty, being medically unfit, or pacemaker insertion, which could have introduced further bias. Consequently, only 31/40 (78%) of patients who underwent baseline assessment were followed up with the day 3±1 scan and of these 21/31 (68%) underwent the 6-month MRI. Finally, inter-study methodological heterogeneity pervades this field of research and must be considered when placing this into the context of previous work.

Conclusions

Our understanding of periprocedural cardioembolic strokes that occur secondary to cardiac interventions is less developed than one might think, and a number of vital questions remain unanswered. In our cohort of patients undergoing TAVI, we identified the posterior circulation and the right hemisphere as particularly vulnerable to cerebral infarctions. These findings contrast with previous reports but are consistent with our knowledge of cardioembolic stroke in theoretical models and other cardiac procedures. Certainly, this has implications for risk-minimisation strategies, particularly when evaluating protective devices designed to prevent the spread of emboli into the cerebral circulation. This is a pertinent issue given the extension of the TAVI procedure to lower-risk patients who have a longer life

expectancy and thus more time for subclinical neurological injury to exert adverse effects.

Author Contribution Statement

JPF, AAW and JFF were involved in the conception and design of the study. JPF also collected and analysed data and drafted the manuscript. AJW, DW, AC, DP, and WS were involved in the design of the study and patient assessment. AB performed statistical analysis and was involved in the drafting of the manuscript. All authors critically reviewed the manuscript and approved the final version.

Disclosure/Conflict of Interest

DW is a consultant to Edwards and Boston Scientific, an investigator for Edwards, Medtronic, Symetis, and Boston Scientific clinical studies, and a past proctor for Edwards. No other author declares competing interests.

References

1.   Fanning JP, Walters DL, Platts DG, et al. Characterization of neurological injury in transcatheter aortic valve implantation: How clear is the picture? *Circulation* 2014; 129: 504-515. DOI: 10.1161/circulationaha.113.004103.

2.   Kapadia SR, Kodali S, Makkar R, et al. Protection Against Cerebral Embolism During Transcatheter Aortic Valve Replacement. *Journal of the American College of Cardiology* 2017; 69: 367-377. DOI: http://dx.doi.org/10.1016/j.jacc.2016.10.023.

3.   Arnold M, Schulz-Heise S, Achenbach S, et al. Embolic cerebral insults after transapical aortic valve implantation detected by magnetic resonance imaging. *JACC Cardiovasc Interv* 2010; 3: 1126-1132.

4.   Ghanem A, Muller A, Nahle CP, et al. Risk and fate of cerebral embolism after transfemoral aortic valve implantation: a prospective pilot study with diffusion-weighted magnetic resonance imaging. *J Am Coll Cardiol* 2010; 55: 1427-1432.

5.   Kahlert P, Knipp SC, Schlamann M, et al. Silent and Apparent Cerebral Ischemia After Percutaneous Transfemoral Aortic Valve Implantation: A Diffusion-Weighted Magnetic Resonance Imaging Study. *Circulation* 2010; 121: 870-878. DOI: 10.1161/CIRCULATIONAHA.109.855866.

6.   Rodes-Cabau J, Dumont E, Boone RH, et al. Cerebral embolism following transcatheter aortic valve implantation: comparison of transfemoral and transapical approaches. *Journal of the American College of Cardiology* 2011; 57: 18-28. Comparative Study Multicenter Study Research Support, Non-U.S. Gov't.

7.   Astarci P, Glineur D, Kefer J, et al. Magnetic resonance imaging evaluation of cerebral embolization during percutaneous aortic valve implantation: comparison of transfemoral and trans-apical approaches using Edwards Sapiens valve. *European Journal of Cardio-Thoracic Surgery* 2011; 40: 475-479. DOI: 10.1016/j.ejcts.2010.11.070.

8.   Uddin A, Fairbairn TA, Djoukhader IK, et al. Consequence of Cerebral Embolism After Transcatheter Aortic Valve Implantation Compared With Contemporary Surgical Aortic Valve Replacement: Effect on Health-Related Quality of Life. *Circulation: Cardiovascular Interventions March* 2015; 8: 3.

9.   Ghanem A, Müller A, Sinning J-M, et al. Prognostic value of cerebral injury following transfemoral aortic valve implantation. *EuroIntervention* 2013; 8: 1296-1306. DOI: 10.4244/EIJV8I11A198.

10.   Fairbairn Ta, Mather aN, Bijsterveld P, et al. Diffusion-weighted MRI determined cerebral embolic infarction following transcatheter aortic valve implantation: assessment of predictive risk factors and the relationship to subsequent health status. *Heart* 2012; 98: 18-23. DOI: 10.1136/heartjnl-2011-300065.

11.   Samim M, Hendrikse J, van der Worp HB, et al. Silent ischemic brain lesions after transcatheter aortic valve replacement: lesion distribution and predictors. *Clinical Research in Cardiology* 2015; 104: 430-438. DOI: 10.1007/s00392-014-0798-8.

12.   Fanning JP, Wesley AJ, Walters DL, et al. Neurological Injury in Intermediate-Risk Transcatheter Aortic Valve Implantation. *Journal of the American Heart Association* 2016; 5. DOI: 10.1161/jaha.116.004203.

13.   Meller SM, Baumbach A, Voros S, et al. Challenges in cardiac device innovation: is neuroimaging an appropriate endpoint? Consensus from the 2013 Yale-UCL Cardiac Device Innovation Summit. *BMC medicine* 2013; 11: 257. DOI: 10.1186/1741-7015-11-257.

14.   van Everdingen KJ, van der Grond J, Kappelle LJ, et al. Diffusion-Weighted Magnetic Resonance Imaging in Acute Stroke. *Stroke* 1998; 29: 1783-1790. DOI: 10.1161/01.STR.29.9.1783.

15.   Kappetein AP, Head SJ, Genereux P, et al. Updated standardized endpoint definitions for transcatheter aortic valve implantation: the Valve Academic Research Consortium-2

consensus document. *European Heart Journal* 2012; 33: 2403-2418. DOI: 10.1093/eurheartj/ehs255.

16.   Pasquier F, Leys D, Weerts JGE, et al. Inter-and Intraobserver Reproducibility of Cerebral Atrophy Assessment on MRI Scans with Hemispheric Infarcts. *European Neurology* 1996; 36: 268-272.

17.   Fazekas F, Chawluk JB, Alavi A, et al. MR signal abnormalities at 1.5 T in Alzheimer's dementia and normal aging. *American Journal of Roentgenology* 1987; 149: 351-356. DOI: 10.2214/ajr.149.2.351.

18.   Fanning JP, Wesley AJ, Wong AA, et al. Emerging spectra of silent brain infarction. *Stroke* 2014; 45 October 7, 2014.

19.   Haussig S, Mangner N, Dwyer MG, et al. Effect of a cerebral protection device on brain lesions following transcatheter aortic valve implantation in patients with severe aortic stenosis: The clean-tavi randomized clinical trial. *JAMA* 2016; 316: 592-601. DOI: 10.1001/jama.2016.10302.

20.   Fanning JP, Platts DG, Walters DL, et al. Transcatheter aortic valve implantation (TAVI): Valve design and evolution. *International Journal of Cardiology* 2013; 168: 1822-1831. DOI: http://dx.doi.org/10.1016/j.ijcard.2013.07.117.

21.   Zarrinkoob L, Ambarki K, Wåhlin A, et al. Blood Flow Distribution in Cerebral Arteries. *Journal of Cerebral Blood Flow & Metabolism* 2015; 35: 648-654. DOI: 10.1038/jcbfm.2014.241.
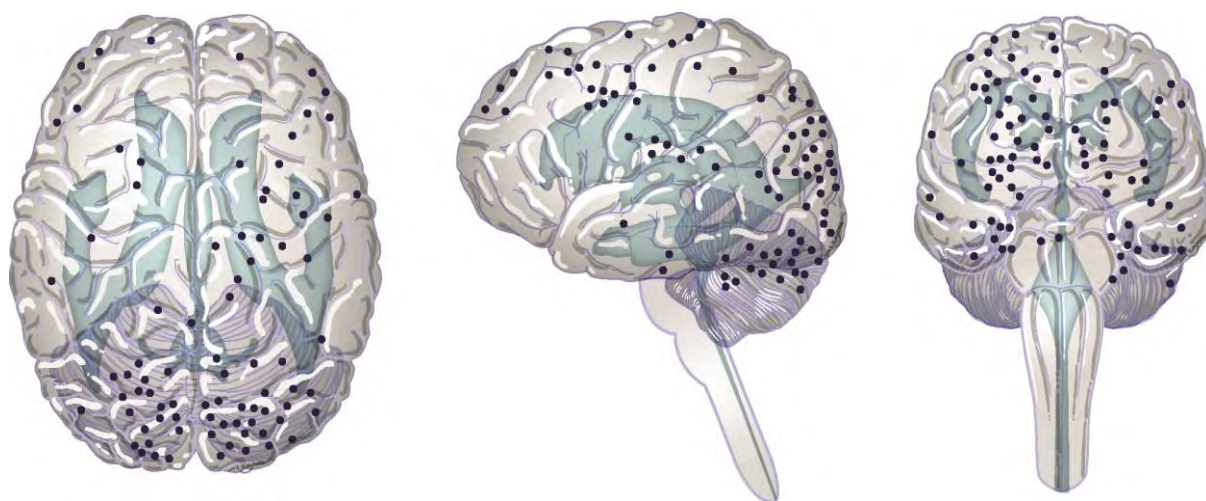
22.   Floßmann E and Rothwell PM. Prognosis of vertebrobasilar transient ischaemic attack and minor stroke. *Brain* 2003; 126: 1940-1954. DOI: 10.1093/brain/awg197.

23.   Kaisti KK, Metsahonkala L, Teras M, et al. Effects of surgical levels of propofol and sevoflurane anesthesia on cerebral blood flow in healthy subjects studied with positron emission tomography. *Anesthesiology* 2002; 96: 1358-1370. 2002/08/10.

24.   Rozet I, Vavilala MS, Lindley AM, et al. Cerebral Autoregulation and CO2

Reactivity in Anterior and Posterior Cerebral Circulation During Sevoflurane Anesthesia.

Anesthesia & Analgesia 2006; 102: 560-564.

25.   Caplan Lr HM. Impaired clearance of emboli (washout) is an important link between

hypoperfusion, embolism, and ischemic stroke. *Archives of Neurology* 1998; 55: 1475-1482.

DOI: 10.1001/archneur.55.11.1475.

26.   Sato K, Sadamoto T, Hirasawa A, et al. Differential blood flow responses to CO2 in

human internal and external carotid and vertebral arteries. *J Physiol* 2012; 590: 3277-3290.

DOI: 10.1113/jphysiol.2012.230425.

27.   Haubrich C, Wendt A, Diehl RR, et al. Dynamic Autoregulation Testing in the

Posterior Cerebral Artery. *Stroke* 2004; 35: 848-852. DOI:

10.1161/01.str.0000120729.99039.b6.

28.   Edvinsson L, Owman C and Sjö¨berg N-O. Autonomic nerves, mast cells, and amine

receptors in human brain vessels. A histochemical and pharmacological study. *Brain

Research* 1976; 115: 377-393. DOI: http://dx.doi.org/10.1016/0006-8993(76)90356-5.

29.   Qureshi AI and Caplan LR. Intracranial atherosclerosis. *The Lancet*; 383: 984-998.

DOI: http://dx.doi.org/10.1016/S0140-6736(13)61088-0.

30.   Carr IA, Nemoto N, Schwartz RS, et al. Size-dependent predilections of cardiogenic

embolic transport. *American Journal of Physiology - Heart and Circulatory Physiology* 2013;

305: H732-H739. DOI: 10.1152/ajpheart.00320.2013.

31.   Barbut D, Grassineau D, Lis E, et al. Posterior Distribution of Infarcts in Strokes

Related to Cardiac Operations. *The Annals of Thoracic Surgery* 1998; 65: 1656-1659. DOI:

http://dx.doi.org/10.1016/S0003-4975(98)00272-0.

32.   Malone M, Prior P and Scholtz CL. Brain damage after cardiopulmonary by-pass: correlations between neurophysiological and neuropathological findings. *Journal of Neurology, Neurosurgery & Psychiatry* 1981; 44: 924-931. DOI: 10.1136/jnnp.44.10.924.

33.   Gilman S. Cerebral Disorders after Open-Heart Operations. *New England Journal of Medicine* 1965; 272: 489-498. DOI: doi:10.1056/NEJM196503112721001.

34.   Brierley JB. Neuropathological findings in patients dying after open-heart surgery. *Thorax* 1963; 18: 291-304.

35.   Hise JH, Nipper ML and Schnitker JC. Stroke associated with coronary artery bypass surgery. *American Journal of Neuroradiology* 1991; 12: 811-814.

36.   Cassie AB, Riddell AG and Yates PO. Hazard of antifoam emboli from a bubble oxygenator. *Thorax* 1960; 15: 22-29.

37.   Kahlert P, Al-Rashid F, Dottger P, et al. Cerebral Embolization During Transcatheter Aortic Valve Implantation: A Transcranial Doppler Study. *Circulation* 2012; 126: 1245-1255.

38.   Kim H-J, Song J-M, Kwon SU, et al. Right-Left Propensity and Lesion Patterns Between Cardiogenic and Aortogenic Cerebral Embolisms. *Stroke* 2011; 42: 2323-2325.

39.   Helenius J, Perkiö J, Soinne L, et al. Cerebral hemodynamics in a healthy population measured by dynamic susceptibility contrast MR imaging. *Acta Radiologica* 2003; 44: 538-546. DOI: 10.1080/j.1600-0455.2003.00104.x.

40.   Stys PK. Anoxic and Ischemic Injury of Myelinated Axons in CNS White Matter: From Mechanistic Concepts to Therapeutics. *Journal of Cerebral Blood Flow & Metabolism* 1998; 18: 2-25. DOI: 10.1097/00004647-199801000-00002.

41.   Arakawa S, Wright PM, Koga M, et al. Ischemic Thresholds for Gray and White Matter: A Diffusion and Perfusion Magnetic Resonance Study. *Stroke* 2006; 37: 1211-1216.

42.   Lansky AJ, Schofer J, Tchetche D, et al. A prospective randomized evaluation of the TriGuard™ HDH embolic DEFLECTion device during transcatheter aortic valve implantation: results from the DEFLECT III trial. *European Heart Journal* 2015; 36: 2070-2078. DOI: 10.1093/eurheartj/ehv191.

43.   Wendt D, Kleinbongard P, Knipp S, et al. Intraaortic Protection From Embolization in Patients Undergoing Transaortic Transcatheter Aortic Valve Implantation. *The Annals of Thoracic Surgery* 2015; 100: 686-691. DOI: http://dx.doi.org/10.1016/j.athoracsur.2015.03.119.

44.   Van Mieghem NM, Van Gils L, Ahmad H, et al. Filter-based cerebral embolic protection with transcatheter aortic valve implantation: the randomised MISTRAL-C trial. *EuroIntervention* 2016; 12: 499-507. DOI: 10.4244/EIJV12I4A84.

Graphical Abstract